TENTH AUSTRALASIAN FLUID MECHANICS
CONFERENCE - UNIVERSITY OF MELBOURNE
11-15 DECEMBER 1989

NUMERICAL PREDICTION AND EXPERIMENTAL MEASUREMENT OF ACOUSTICS AND FLOW IN A DUCT WITH BAFFLES

A.N. STOKES[1], M.C. THOMPSON[2], K. HOURIGAN[2] and M.C. WELSH[2]

[1]CSIRO Division of Mathematics and Statistics
Private Bag 10, Clayton, Victoria 3168, AUSTRALIA

[2]CSIRO Division of Building, Construction and Engineering
P.O. Box 56, Highett, Victoria 3190, AUSTRALIA

ABSTRACT

The flow around baffles in a rectangular duct, the excitation of a resonant mode of the duct, and the feedback of the sound onto the flow separation are investigated both computationally and experimentally. It is shown that the shedding of large-scale vortex structures in the shear layer between an upstream and a downstream set of baffles is locked to the sound field when a resonance is excited. In addition, the flow velocity is critical in determining whether these vortices generate or absorb acoustic power as they pass the downstream set of baffles.

1. INTRODUCTION

Nomoto and Culick (1982) published data showing vortex shedding exciting acoustic resonances in rectangular ducts containing two pairs of baffles; resonances were predominantly the organ pipe modes of the duct. They observed the same resonant acoustic mode being excited over several different ranges of flow velocity. The different ranges are characterised by different numbers of vortices being observed between the baffles at any particular phase of the acoustic cycle.

Stokes and Welsh (1985) have described the acoustic sources associated with the flows around a rectangular plate and extended the theory to the case of flow in a duct with baffles (Welsh and Stokes, 1985), which is shown in Figure 1.

The aim of this paper is to describe the acoustic sources in the duct containing the baffles in terms of the flow and the acoustic field near the baffles using Howe's (1975) theory of aerodynamic sound. The flow is represented as the sum of a steady potential contribution, flow induced by point vortices, and an oscillating component representing the acoustic field. The predictions are compared with experimental results. Only the case for the simplest acoustic mode is described, corresponding to the one with a wavelength approximately equal to the length of the working section.

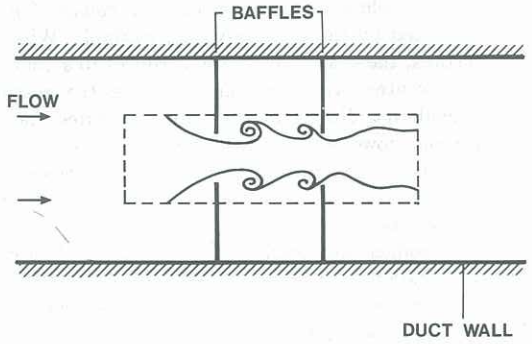

Figure 1: Schematic of experimental working section. The dotted line indicates the region shown in Figures 4 and 5.

2. THEORY

2.1 Acoustic Field

The resonant acoustic mode corresponds to a principally longitudinal duct mode modified by the sets of baffles. For the flows of interest, the Mach number is small and the acoustic pressure p approximately satisfies the wave equation. Also, since the solutions are standing waves, separation of variables can be used and the spatial variation of acoustic pressure satisfies the Helmholtz equation. The acoustic local velocity vectors are shown in Figure 2 for the region near the baffles, and a particular point in the cycle. During the acoustic cycle, the magnitude of the velocities changes continuously, but the direction only changes when it periodically reverses. The finite element method is used to find the eigenmodes, as described in Thompson *et al.* (1988).

2.2 Flow Modelling: Vortex Cloud Model

The flow is modelled as a two-dimensional inviscid incompressible flow, irrotational everywhere except at the centres of elemental vortices. The shedding of vorticity is modelled by the creation and release of elemental vortices, which are subsequently convected under the influence of other vortices and the irrotational flow. The surface vorticity method used and the shedding of elemental vortices into the flow is described in more detail in Thompson *et al.* (1988) and Lewis (1981).

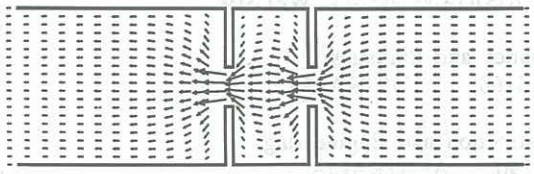

Figure 2: Velocity vectors showing the local direction of the acoustic field in the vicinity of the baffles.

2.3 Acoustic Power Generation

According to Howe's theory of aerodynamic sound (1975), the acoustic power P generated by a vortex moving at velocity $\underline{v}$ through a sound field having a local particle velocity $\underline{u}$ can be obtained by integrating, over the spatial neighborhood of the vortex, the scalar triple product $\underline{\omega} \times \underline{v} \cdot \underline{u}$ where $\underline{\omega}$ is the local vorticity. The value of $\underline{u}$ is given by the solution of the Helmholtz equation and the values of $\underline{v}$ and $\underline{\omega}$ are provided by the discrete-vortex method. With discrete vortices, the spatial integration reduces to summation over vortex centres, with some care taken over the treatment of the singularity. Note that the factor $\underline{u}$ ensures that this instantaneous power will be oscillatory; nett energy results when there is an imbalance between the contributions of the positive and negative parts of the cycle. Note too that there will be no acoustic power at all if any two of the vectors in the triple product are parallel. This is important, because in many situations, like the present, the acoustic and mean flow velocities are forced by the boundary conditions to follow generally parallel paths.

3. EXPERIMENTAL EQUIPMENT

A test rig was assembled by connecting the working section of an open circuit draw through wind tunnel to the outlet of an open jet wind tunnel.The tunnel is described in detail in Welsh *et al.* (1990). It was used to study the resonant acoustic process excited by the flow over baffles using a geometry in the working section similar to that of Nomoto and Culick (1982). A microphone was mounted flush with the inner surface of the duct wall between the baffles to measure the sound pressure level. Smoke could be introduced into the flow upstream of the baffles for flow visualisation, and high speed flash photography which could be timed to coincide with events in the sound cycle was used to record the results.

4. RESULTS AND DISCUSSION

The acoustic mode is essentially a perturbation, induced by the baffles, of the lowest frequency open-duct mode. The particles generally oscillate in a horizontal direction, except near the plates, where the velocities, as shown in Figure 2, have a significant vertical component.

The sound pressure level of the signal detected by the microphone when resonance occurs shows peaks at acoustic Strouhal numbers (acoustic frequency normalized with respect to distance between baffles and mean velocity of the flow well upstream of baffles) of 4.7, 7.7 and 11.0. These acoustic resonances all have the same frequency (≈100 Hz)

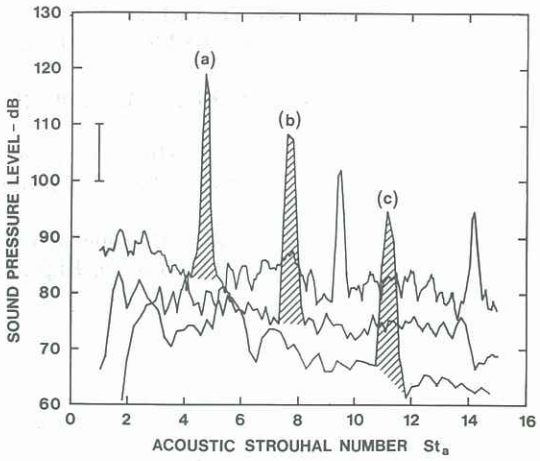

Figure 3: Power spectra measured by the wall microphones at upstream flow velocities of (a) 2.7 m/s, (b) 1.7 m/s, (c) 1.18 m/s. The frequencies are scaled to the acoustic Strouhal number. Each measurement was taken at an acoustic resonance. The shaded peaks correspond to the acoustic resonant frequency, the other obvious peaks are harmonics.

and correspond to the resonant mode described above in 2.1. The spectra are shown in Figure 3.

The flow observed by smoke visualisation was found to be absolutely synchronised with the sound field whenever resonance was established. Multiple flash photographs synchronised with the sound could be superimposed; these are shown in Figure 5 for the flow between the baffles at the acoustic Strouhal numbers 4.7, 7.7 and 11.0, for which the resonant acoustic mode reaches local peaks in the sound pressure level. The photographs show, respectively, one, two and three pairs of vortices between the baffles. In each case, the photograph is taken at the same phase of the sound cycle. In each case, too, there is a vortex just about to pass the second baffle.

The synchronisation clearly indicates a feedback of the resonant sound onto the flow separating at the upstream set of baffles, leading to the vortex shedding being locked in frequency to the excited resonant mode.

'Snapshots' showing vortex positions predicted by the discrete vortex method are given for approximately the same Strouhal numbers in Figure 5. The same pattern of numbers of vortex clusters is observed, although at the highest Strouhal number (lowest velocity) the third cluster is indistinct.

For the predicted discrete vortex motion, the scalar triple product of section 2.3 can be calculated, and is plotted in Figure 6 integrated over the whole flow, as a function of time. The two Strouhal numbers chosen, 4.7 and 6.0, correspond to cases of respectively maximum and minimum energy available for transfer to the acoustic field. At a Strouhal number of 4.7, the space integral of the triple product is positive for almost the whole cycle, and therefore so is the total energy per cycle, which is the integral over time. At the Strouhal number of 6.0, the opposite is true.

The predicted acoustic energy generated per acoustic cycle over a range of Strouhal numbers is shown in Figure 7. The points correspond to integrals over one cycle of functions cor-

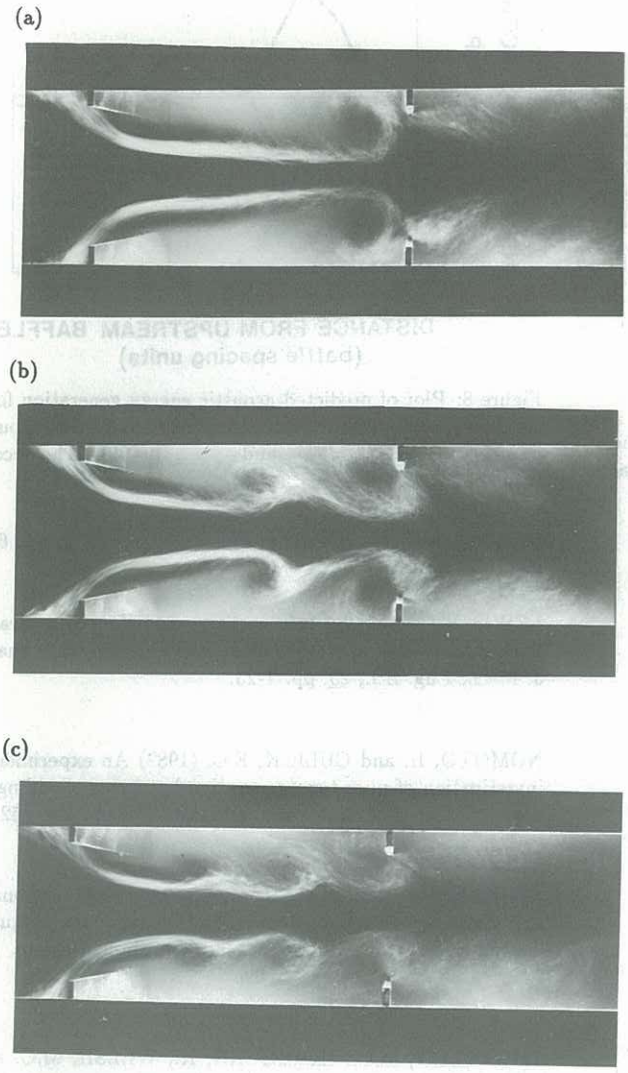

Figure 4: Smoke patterns occurring during resonance showing one, two and three pairs of vortices between the baffles. The Strouhal numbers are 4.7, 7.7 and 11.0, respectively.

responding to those plotted in Figure 6 for two particular Strouhal numbers. The Strouhal numbers at which peaks in acoustic energy generation occur are found to coincide well with the observed values.

An interpretation of the effect shown in Figure 6 can be obtained by plotting the integral of the scalar triple product over the area occupied by one large vortex structure. The result is shown in Figure 8, plotted not against time, but the distance moved by the centroid of the vortex. The velocity of the vortex is reasonably uniform, so the plot as a function of time is similar. The oscillations forecast in Section 2.3 occur, but are quite lop-sided about the zero mean, which is to be expected, since extreme cases of power generation and non-generation where chosen.

For a Strouhal number of 4.8, a large-scale vortex contributes a net positive power as it passes the downstream set of baffles; for a Strouhal number of 6.0, a net negative power contribution results. The reason is the phase difference in the acoustic particle velocity. At the first baffle the vortices are formed at a particular phase of the sound cycle; the phase at

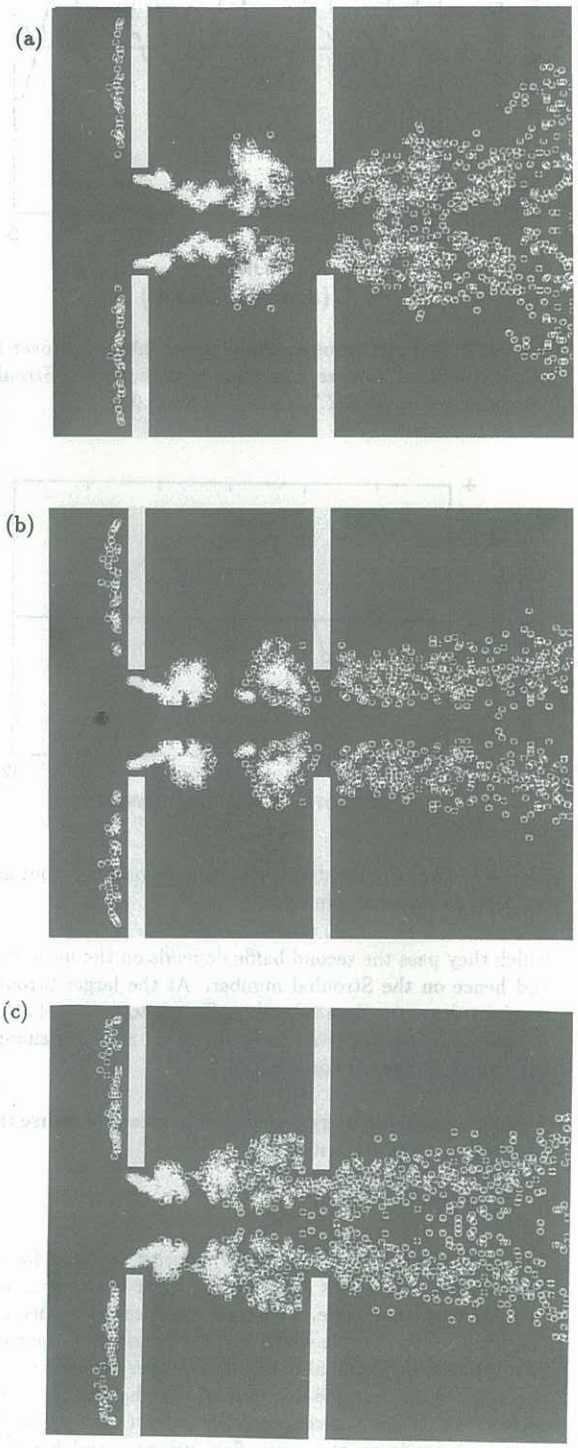

Figure 5: Plots of discrete vortex positions for Strouhal numbers corresponding to local maximum acoustic energy output. From top to bottom, St = 4.8, 7.7 and 11.0, respectively.

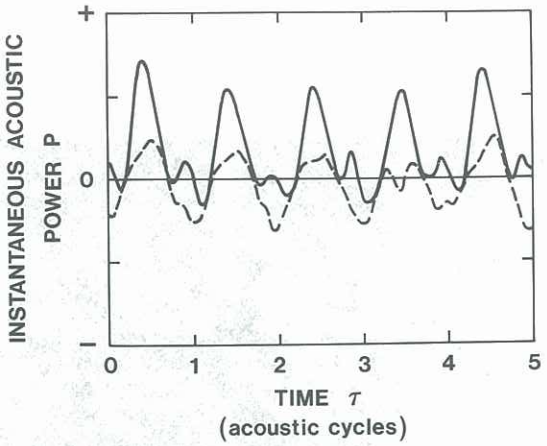

Figure 6: Instantaneous acoustic power integrated over the whole predicted flow, as a function of time, for the Strouhal numbers: ——, St = 4.7; and - - - , St=6.0

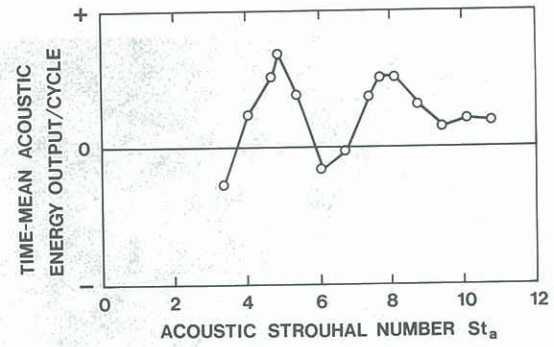

Figure 7: Plot of predicted mean acoustic power output as a function of Strouhal number.

which they pass the second baffle depends on the mean flow, and hence on the Strouhal number. At the larger Strouhal number, the extra time taken is sufficient to ensure that the acoustic particle velocities have reversed, and this changes the sign of the power contribution.

A negative acoustic energy contribution means of course that no resonance can be sustained.

5. CONCLUSION

The sound field perturbs the flow velocity near the baffles, and this has a feedback effect on the shear layer separating from the upstream baffle. This causes vortices to be shed at a point in the sound cycle which is not dependent on the mean flow velocity, or Strouhal number. Whether acoustic energy is generated or absorbed depends on the phase of the sound cycle at which the vortices reach the downstream baffle; this in turn depends on the mean flow velocity, and hence on the Strouhal number. This explains why there are discrete ranges of Strouhal number at which resonance occurs, and why each range is characterised by the number of vortices observed between the baffles at any time.

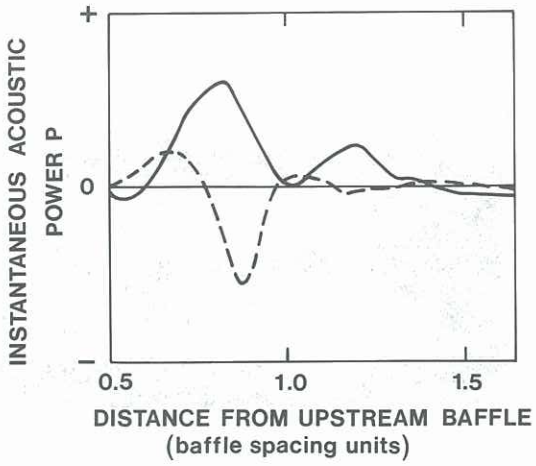

Figure 8: Plot of predicted acoustic energy generation for a single vortex cloud as it passes the second baffle for Strouhal numbers: ——, St = 4.7; and - - - , St=6.0. The second baffle is positioned at $x = 1$.

REFERENCES

HOWE, M.S. (1975) Contributions to the theory of aerodynamic sound, with application to excess jet noise and the theory of the flute. Journal of Fluid Mechanics, 71, pp. 625-673.

LEWIS, R.I. (1981) Surface vorticity modelling of separated flows from two-dimensional bluff bodies of arbitrary shape. J. Mech. Eng. Sci., 23, pp. 1-23.

NOMOTO, H. and CULICK, E.C. (1982) An experimental investigation of pure tone generation by vortex shedding at a duct. Journal of Sound and Vibration, 84, pp. 247-252.

STOKES, A.N. and WELSH, M.C. (1985) Flow - resonant sound interaction in a duct containing a plate, Part II: square leading edge. Journal of Sound and Vibration, 104, pp. 55-73.

THOMPSON, M.C., HOURIGAN, K., WELSH, M.C. and SOH, W.K. (1988) Sources of acoustic resonance in a duct with baffles. Fluid Dynamics Research, 3, pp 349-352..

WELSH, M.C., HOURIGAN, K., WELCH, L.W., DOWNIE, R.J., THOMPSON, M.C., and STOKES, A.N. (in press). Acoustics and experimental methods: The influence of sound on flow and heat transfer. Experimental Thermal and Fluid Sci.

WELSH, M.C. and STOKES, A.N. (1985) Transient vortex modelling for flow-induced acoustic resonances near cavities or obstructions in ducts. IUTAM Symposium, Lyon, France, pp. 499-505.